PERGAMON

Journal of Structural Geology 24 (2002) 593–607

JOURNAL OF STRUCTURAL GEOLOGY

www.elsevier.com/locate/jstrugeo

Interpreting the geologic map expression of contractional fault-related fold terminations: lateral/oblique ramps versus displacement gradients

M. Scott Wilkerson[a,*], Ted Apotria[b], Tammer Farid[a]

[a]*DePauw University, Department of Geology and Geography, 602 S. College Ave., Greencastle, IN 46135, USA*
[b]*ExxonMobil Exploration Company, 233 Benmar Street, Houston, TX 77060, USA*

Received 18 July 2000; revised 27 February 2001; accepted 1 March 2001

Abstract

Fault-related folds in contractional settings do not extend indefinitely, but rather commonly terminate as plunging anticlines near the tips of the genetically-related fault. Geologists often attribute the formation of such terminations to loss of slip on the underlying fault (i.e. a displacement gradient), to changes in fault geometry in which the fault laterally changes stratigraphic position along strike (i.e. a lateral/oblique ramp), or to some combination of these mechanisms. Discerning between these formative mechanisms solely through the interpretation of the geologic map expression of the termination can be difficult because of the subjective nature of the criteria used (e.g. lateral/oblique ramps often are interpreted at terminations where folds plunge at 'steep' angles, where hanging wall cutoff lines trend at 'high' angles to fault strike, where stratigraphic contacts trend at 'high' angles to fault strike, etc.).

We created pseudo-three-dimensional model terminations of individual fault-related folds using both displacement gradients and lateral/oblique ramps to determine if unique characteristics in their map expressions exist. We show that map patterns of folds produced by a displacement gradient along a thrust fault of constant geometry are similar to map patterns of folds produced by constant slip on a thrust fault with a lateral/oblique ramp. Specifically, our modeling results suggest that (1) simple fault-bend folds that plunge less than 20° and simple fault-propagation folds that plunge less than 50° at their terminations can be created by both displacement gradients and lateral/oblique ramps; angles greater than these values suggest that a lateral/oblique ramp may be involved in forming the termination, (2) hanging wall cutoff lines at terminations that trend at angles less than about 35° to fault strike for simple fault-bend and fault-propagation folds also may be produced by both displacement gradients and lateral/oblique ramps; higher angles likely indicate the presence of a lateral/oblique ramp at the termination, (3) the angle at which stratigraphic contacts trend to the fault strike cannot be used to uniquely identify displacement gradients or lateral/oblique ramps for simple fault-related folds, (4) stratigraphic separation diagrams can indicate the presence of ramps in the thrust sheet, but do not uniquely differentiate between frontal ramps with displacement gradients and lateral/oblique ramps, and (5) actual changes in fault orientation (after topographic influences have been taken into account), by definition, indicate a lateral/oblique ramp. In reality, most natural fault-related fold terminations probably share components of both displacement gradients and lateral/oblique ramps, with each structure possessing contributions from each mechanism.

Keywords: Fold terminations; Lateral/oblique ramps; Displacement gradients; Fault-related folds

1. Introduction

Structural geologists have long recognized that contractional fault-related folds in fold-thrust belts do not extend indefinitely (e.g. Bielenstein, 1969; Dahlstrom, 1970; Elliott, 1976; Wheeler, 1980; Coward and Potts, 1983; Liu and Dixon, 1991; Dixon and Liu, 1992; Wilkerson, 1992; Wilkerson and Wellman, 1993; Prine, 1997; Fermor, 1999). These folds commonly reach their greatest amplitude near the central portion of a genetically-related thrust fault and lose amplitude toward the lateral tips of the fault. Near these lateral fault tips, both the fault and the related fold terminate, producing a plunging anticline (Fig. 1).

Geologists generally attribute the termination of fault-related folds to one of three mechanisms: (1) loss of slip (i.e. a displacement gradient) on the underlying frontal fault ramp, (2) changes in fault geometry in which the fault cuts laterally upsection along strike from a deeper detachment to a shallower level to form either a lateral or oblique ramp, or (3) a combination of both mechanisms (see Table 1 for examples). Each of these ramp types (frontal, lateral, and oblique) occur where footwall strata are truncated by the fault and are defined with respect to the overall transport direction (Fig. 2). Specifically, frontal ramps strike

* Corresponding author. Tel.: +1-765-658-4666; fax: +1-765-658-4732.
E-mail addresses: mswilke@depauw.edu (M. Scott Wilkerson), ted.g.apotria@exxonmobil.com (T. Apotria).

0191-8141/02/$ - see front matter
PII: S0191-8141(01)00111-0

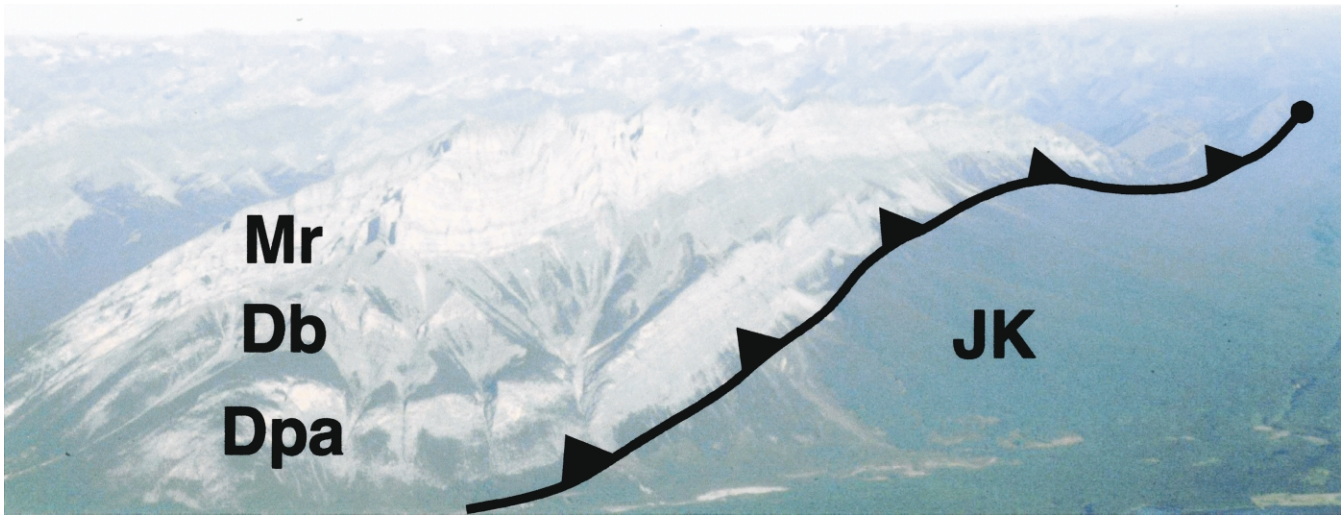

Fig. 1. Photo of the northern termination of the Rundle thrust in Alberta, Canada. View is to the northwest. Devonian Palliser (Dpa), Devonian Banff (Db), and Mississippian Rundle Group (Mr) rocks in the hanging wall of the Rundle Thrust define a NW-plunging anticline above Jurassic and Cretaceous (JK) footwall rocks. The lateral termination of the surface trace of the Rundle thrust ends at the right edge of the photo (dark circle), and the town of Banff is just off the left edge of the photo.

perpendicular to the transport direction, lateral ramps strike parallel to the transport direction, and oblique ramps strike at an acute angle to the transport direction (Fig. 2). For the purposes of this paper, we will use the term 'lateral/oblique ramp' interchangeably with lateral ramp because, although differences between the two undoubtedly exist, many of the comparisons that we make between pure lateral ramps and displacement gradients hold true for oblique ramps as well.

In the absence of seismic reflection data, well control, or detailed footwall stratigraphic cutoff information, geologists have to infer the dominant mechanism or the relative contributions of the two mechanisms causing the structure to terminate using only surface geology data. Interpreting such surface geology data, especially in areas where fault-related folds may be later tilted and eroded, can be difficult and often results in conflicting interpretations. These different interpretations develop because map-based criteria for interpreting the formative mechanism of fault-related fold terminations are subjective and criteria for distinguishing between terminations that form due to loss of displacement along strike and those due to lateral/oblique ramps have not been adequately described.

This study evaluates geological observations commonly used to infer that a lateral/oblique ramp in the underlying fault produces a fault-related fold termination. To facilitate this evaluation, we created pseudo-three-dimensional model terminations for each mechanism of formation assuming simple fault-bend (flat–ramp–flat; e.g. Suppe, 1983) and fault-propagation fold (flat–ramp; e.g. Suppe and Medwedeff, 1990) geometries. Analysis of these model terminations helps (1) to constrain subjective criteria used to substantiate a given interpretation, and (2) to determine if unique characteristics exist that may be used as a predictive tool in interpreting natural structures.

2. Evaluation of criteria supporting a lateral/oblique ramp interpretation for fault-related fold terminations

Five lines of evidence, either individually or in combination, often are used to support the interpretation of a lateral/oblique ramp for a particular termination; they are:

- folds at the termination plunge at 'steep' angles,
- hanging wall cutoff lines trend at 'high' angles to fault strike,
- stratigraphic contacts trend at 'high' angles to fault strike,
- stratigraphic separation diagrams display 'abrupt' changes near terminations, and
- faults exhibit actual changes in orientation.

In the following paragraphs, we investigate each of these criteria in detail.

2.1. Folds at termination plunge at 'steep' angles

Published interpretations of fault-related fold terminations often correlate areas where the fold plunges at 'steep'angles with lateral/oblique ramps in the underlying fault (e.g. Castonguay and Price, 1995; Prine, 1997). 'Steep' is a subjective term; most commonly a fault-related fold is considered to have a 'steep' plunge at its termination if the plunge (1) is considerably larger than plunges observed along the strike of that particular hanging wall fold/thrust sheet, and/or (2) is considerably larger than plunges observed on neighboring folds/thrust sheets.

We help place constraints on 'steep' by calculating maximum plunges for fault-related fold models that terminate with only a displacement gradient and no change in fault geometry along strike. To do so, we follow the approach of

Table 1
Summary of contractional fault-related fold termination studies (direction of termination shown in parentheses: N = north, S = south, E = east, W = west, SSD = stratigraphic separation diagram)

Location	Reference	Main Interpretation	Evidence
Front Ranges, Canada (S) McConnell thrust	Douglas (1958)	lateral ramp	tear faults, abrupt hanging-wall thickness changes on geologic map, steep plunge
Front Ranges, Canada (N) Rundle thrust	Bielenstein (1969)	lateral ramp	steep segment on SSD, HW truncations on geologic map
Front Ranges, Canada (N) Exshaw thrust	Gardner & Spang (1973)	displacement "transfer"	comparison of geologic map pattern w/ physical models
Front Ranges, Canada (N) Lewis thrust	Stockmal (1979)	displacement "transfer"	gradual loss of displacement transferred to nearby structures (faults and folds)
Appalachian Mt., VA (N) Saltville thrust	House & Gray (1982)	displacement "transfer"	gradual loss of displacement on geologic map & SSD, physical models & mesoscopic structures suggest transfer from faulting to folding
Sawtooth Range, MT (N) Teton River transfer zone	O'Keefe & Stearns (1982)	displacement "transfer" (w/ minor "strike" ramps)	termination geometry on SSD's, comparison of geologic map pattern w/ physical models
Sawtooth Range, MT (N) French & Old French thrusts (S) Diversion thrust	Goldburg (1984)	"transverse"ramp (w/ displacement "transfer")	HW truncations on geologic map, along-strike displacement changes shown on displacement-distance diagram
Idaho-Wyoming-Utah fold-thrust belt Crawford and Meade thrust sheets	Evans & Craddock (1985)	"displacement transfer" accommodated by a lateral ramp	SSD's and balanced cross sections
Wasatch Range, UT Ogden duplex	Schirmer (1988)	lateral ramp	construction of hanging-wall sequence diagrams from geologic map
Variscan thrust belt, S. Wales (E) Tutt Head thrust zone	Hyett (1990)	lateral ramp	mapping of stratigraphic cutoff
N/A synthetic model structures	Wilkerson et al. (1991)	displacement gradient lateral/oblique ramps	creation of pseudo-3D geometric models from serial balanced cross sections
Laramide basement-involved structures, Western US	Ratliff (1992)	displacement gradient	comparison of structure-contour maps of pseudo-3D models with natural structures
Golden Gate Range, NV (N) Golden Gate thrust	Armstrong & Bartley (1993)	displacement gradient	displacement and fault geometry measured from outcrop exposures
Appalachian Mts., VA (N) Saltville & St. Clair thrusts	Couzens & Dunne (1994)	displacement "transfer"	micro- and mesostructural data suggest transfer to floor thrust and to fold
Sevier fold-thrust belt, WY (N) South Fork thrust	Apotria (1995)	oblique ramp	fault orientation changes in HW and FW, mesoscopic fabrics & strain analysis suggest corresponding rotations
Front Ranges, Canada (S) Misty thrust	Castonguay & Price (1995)	oblique ramp	"abrupt" change in HW detachment level shown on geologic maps and SSD, fold trending obliquely to fault strike
Betic Cordillera, Spain unnamed thrust	Frizon de Lamotte et al. (1995)	lateral ramp	lateral extension of roof sequence, fold trend sub-parallel to transport direction
Front Ranges, Canada (S) Misty thrust	Hennings et al. (1996)	oblique ramp	"abrupt" change in HW detachment level, fold trending obliquely to fault strike
Front Ranges, Canada (N) Rundle thrust & (S) Misty thrust	Prine (1997)	oblique ramp	creation of pseudo-3D geometric models from map and cross-sectional data
Front Ranges, Canada (S) Sulphur Mt. thrust	Prine (1997)	displacement gradient (w/ minor fault bend)	creation of pseudo-3D geometric models from map and cross-sectional data
Foothills & Front Ranges, Canada (S) Bighorn, Brazeau, Highwood, Turner Valley, McConnell/Livingstone, Misty, & Boule thrusts (N) Turner Valley & Jumping Pound thrusts	Fermor (1999)	lateral ramp	seismic interpretation and derivative cutoff line maps
Foothills & Front Ranges, Canada (N) McConnell, Sulphur Mt./Colin, Lewis, & Borgeau thrusts	Fermor (1999)	displacement gradient	seismic interpretation and derivative cutoff line maps
Eastern Cordillera, Colombia Medina anticline	Rowan & Linares (2000)	displacement gradient and oblique ramp	seismic interpretation, axial-surface mapping, pseudo-3D geometric models
Front Ranges, Canada (N) Rundle thrust	Price (in review)	lateral ramp	tear fault relationships and oblique fold at Cascade Mt. on geologic map

Wilkerson et al. (1991), who derived equations describing the geometry of pseudo-three-dimensional fault-related fold terminations for simple fault-bend (Suppe, 1983) and fault-propagation (Suppe and Medwedeff, 1990) folds with linear displacement gradients and constant fault geometries.

For a simple flat–ramp–flat, fault-bend fold termination (Fig. 3), the height z of any folded surface above its regional level is:

$$z = s\sin\Theta \tag{1}$$

where s is slip at the trailing edge of the fault-bend fold, Θ is the footwall ramp cutoff angle, and z cannot exceed the

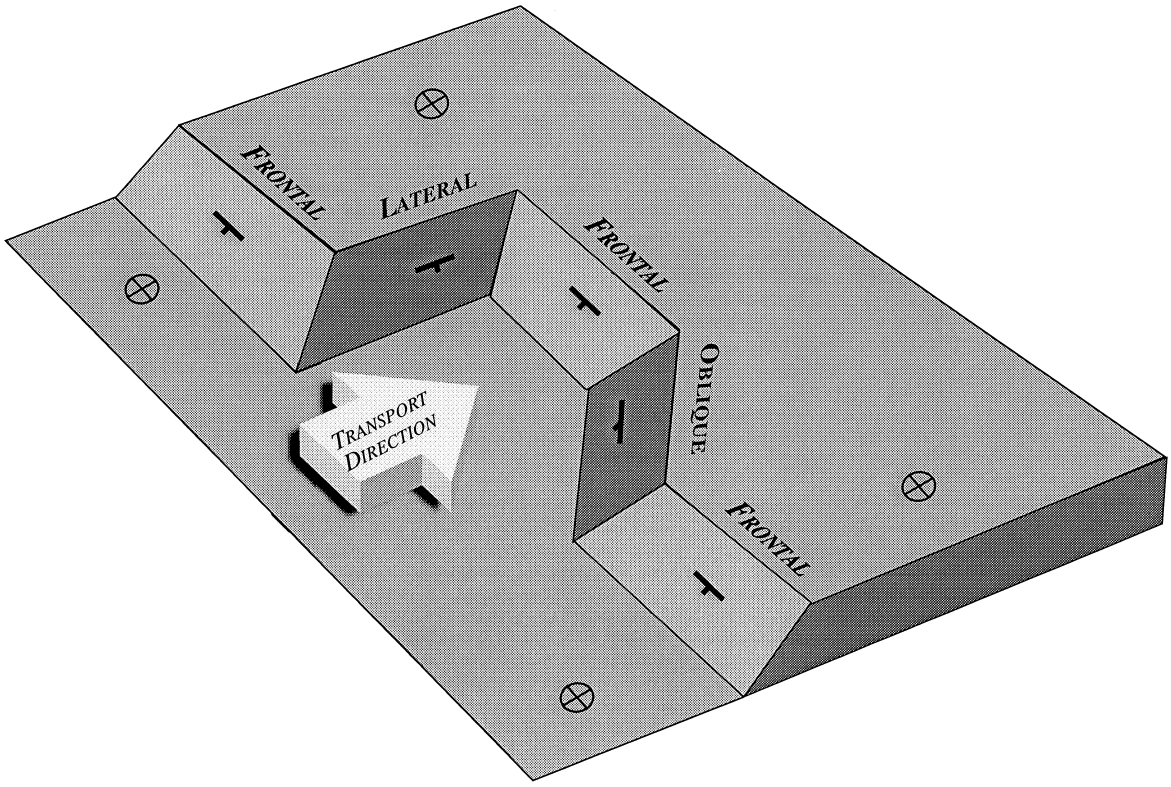

Fig. 2. Block diagram of an idealized footwall with frontal, oblique, and lateral fault ramps (modified from Wilkerson and Marshak, 1997). See text for definitions.

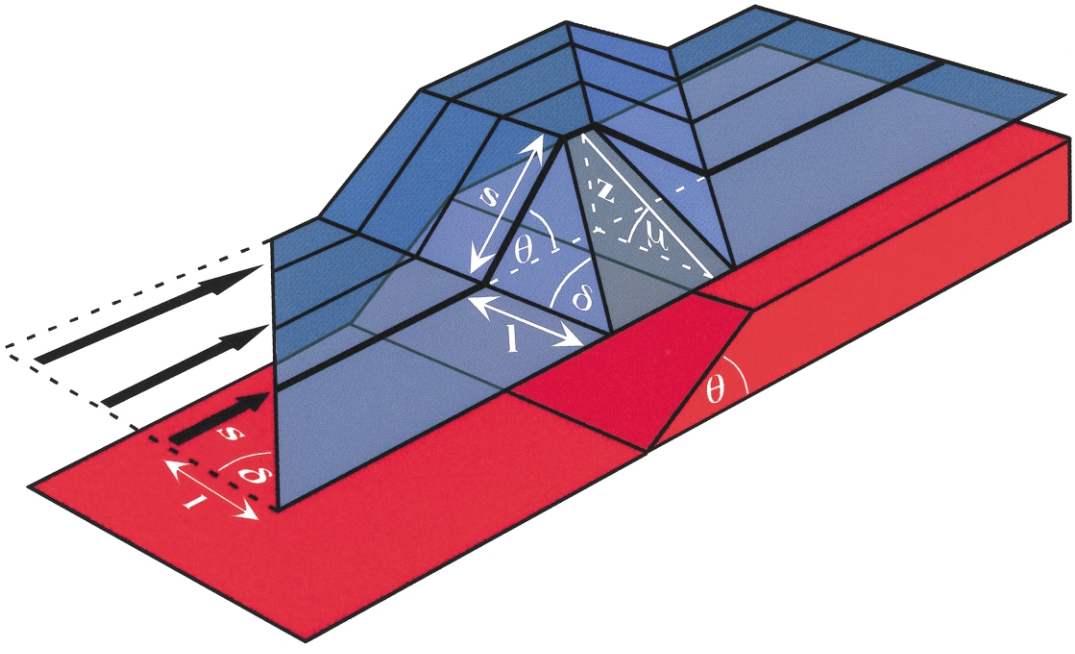

Fig. 3. Block diagram of a model fault-bend fold that possesses a constant fault geometry and a trailing-edge displacement gradient (i.e. a systematic, strike-parallel loss of displacement along the strike of a fault, which, in this paper, is assumed to be linear and represented by the angle δ). For the outlined cross section, z is the height of the folded surface above its regional level, s is slip at the trailing edge, l is the strike-length distance from the section with displacement s to the termination, Θ is the footwall ramp cutoff angle, and μ is the plunge of the folded surface at the termination. Note that s and δ at the trailing edge of the diagram are distorted in this perspective view.

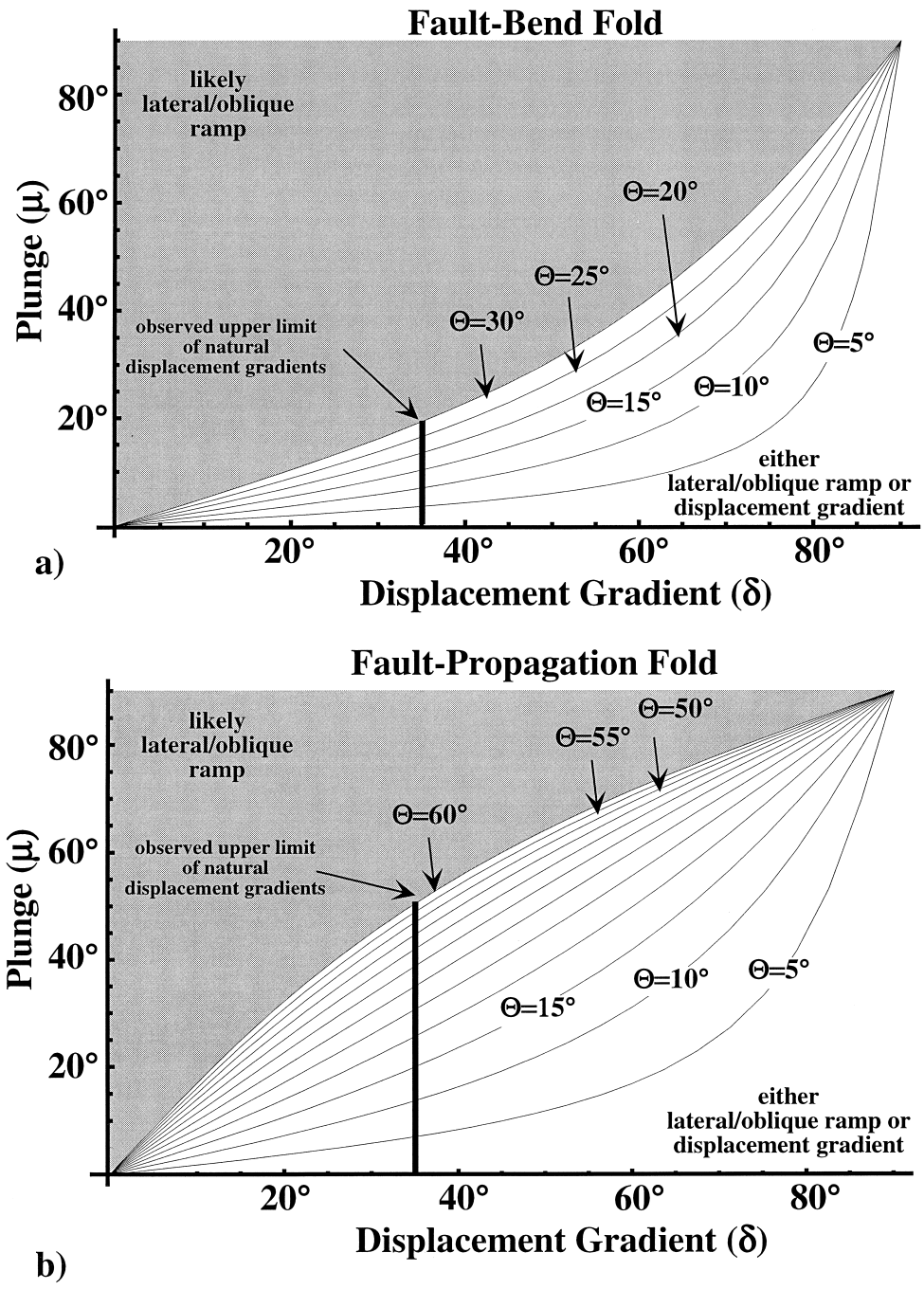

Fig. 4. Graphs plotting fold plunge μ as a function of displacement gradient δ and footwall ramp cutoff angle Θ for simple (a) fault-bend and (b) fault-propagation folds with constant fault geometry. Lines of equal Θ are shown at 5° increments up to their theoretical maximums of 30° for simple fault-bend folds (Suppe, 1983) and 60° for simple fault-propagation folds (Suppe and Medwedeff, 1990). The line at $\delta = 35°$ is an approximate maximum displacement gradient observed for continuous, non-metamorphic thrust sheets (Wilkerson, 1992). Fold plunges that plot below the shaded region and left of the line could theoretically be the product of either a displacement gradient or a lateral/oblique ramp, whereas plunges that plot within the shaded region are more likely caused by lateral/oblique ramps.

footwall ramp height. The slip s also can be used to define the linear displacement gradient δ on the trailing edge of the fault-bend fold:

$$\tan\delta = \frac{s}{l} \tag{2}$$

where s is slip at the trailing edge of the fault-bend fold and l is the along-strike length of the fold over which the linear displacement gradient is maintained (Fig. 3). With this information, the plunge of the fold μ then can be described by:

$$\tan\mu = \frac{z}{l} \tag{3}$$

Rearranging and substituting Eqs. (1) and (2) into Eq. (3),

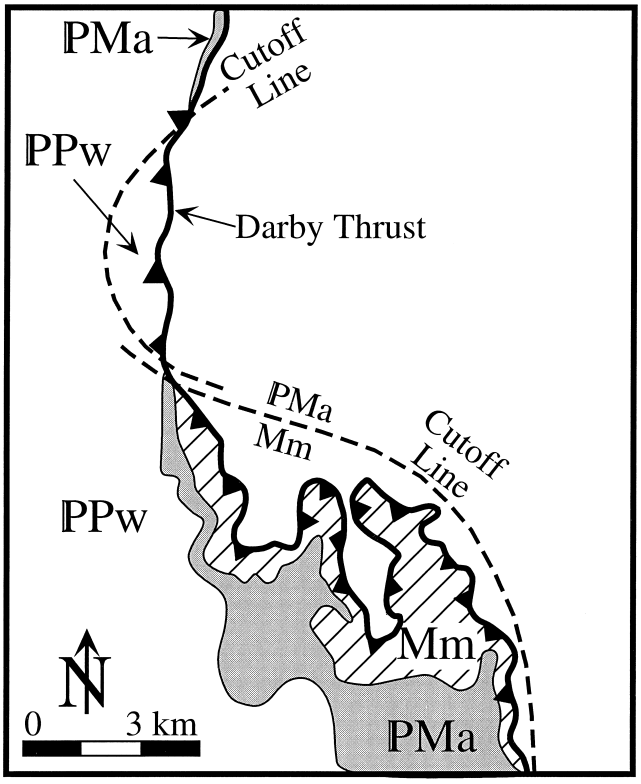

Fig. 5. Cutoff-line map from the Darby thrust, Wyoming, north of Mt. McDougal (modified from Woodward, 1987). Cutoff lines involving three units (Madison Group—Mm, Amsden Formation—PMa, and Wells Formation—PPw) trend at high angles (>33–35°) to the NNW fault strike of the Darby thrust, suggesting a lateral/oblique ramp.

we arrive at the final expression relating plunge of a simple fault-bend fold termination to the displacement gradient and footwall ramp cutoff angle:

$$\tan\mu = \sin\Theta\tan\delta \quad (4)$$

We can similarly derive an expression for the plunge of a simple flat–ramp, fault-propagation fold termination, except that z now is twice as large as that for a fault-bend fold (this relationship occurs because the anticlinal axial surface propagates an amount equal to twice the fault slip). The final expression relating plunge of a simple fault-propagation fold termination to displacement gradient and footwall ramp cutoff angle is:

$$\tan\mu = 2\sin\Theta\tan\delta \quad (5)$$

Eqs. (4) and (5) are plotted in Fig. 4 for a range of footwall ramp cutoff angles (0–30° for fault-bend folds (Suppe, 1983); 0–60° for fault-propagation folds (Suppe and Medwedeff, 1990)) and for displacement gradients ranging from 0 to 90°. In nature, however, displacement gradients for non-metamorphic thrust sheets do not possess such a broad range. Wilkerson (1992) cataloged shortening versus strike-length relationships for individual non-metamorphic thrust sheets in North America in order to constrain natural ranges for displacement gradients. He found that displacement gradients did not exceed 35–40° (a bulk shear strain of 0.70–0.84) for continuous thrust sheets without forming prominent cross-strike features in the hanging wall thrust sheet. If we assume that 35° is a maximum displacement gradient for natural non-metamorphic thrust sheets, then maximum plunges may reach up to 20 and 50° for simple fault-bend and fault-propagation folds, respectively (below the shaded regions and to the left of the lines of the graphs in Fig. 4; depending on fault ramp dip). In contrast, plunges for lateral ramps with constant displacement are equal in magnitude and opposite in direction to the dip of the lateral ramp because the plunge is only related to changes in the fault geometry (thereby allowing plunges to range from 0 to 90°, in theory).

Although caution must be exercised in applying model results to natural structures, these results suggest that interpretations of terminations of natural structures based solely on 'steep' plunges are ambiguous for individual fault-bend folds that plunge ≤20° and for individual fault-propagation folds that plunge ≤50° (depending on fault ramp dip). Greater plunges for individual fault-bend or fault-propagation fold terminations in the absence of additional imbrications/complications suggest that a lateral/oblique ramp is likely involved.

2.2. Hanging wall cutoff lines trend at 'high' angles to fault strike

Cutoff lines are lines of intersection between stratigraphic contacts and a fault surface; matching cutoff lines exist (or once existed) in every hanging wall and footwall for every mappable contact. Direct measurement of cutoff lines at fault-related fold terminations often is difficult, but can be greatly facilitated by small erosional re-entrants (Woodward, 1987; Fig. 5). In these re-entrants, multiple occurrences of the same cutoff allow the interpreter to ignore the irregular erosional trace of the fault and to connect these cutoffs to form stratigraphic cutoff lines (Fig. 5, dashed lines). The orientation of these lines then can be objectively evaluated with respect to the transport direction and true fault strike.

Geologists often interpret cutoff lines that trend at 'high' angles to fault strike as suggesting the presence of a lateral/oblique ramp, whereas cutoff lines that trend approximately parallel to the strike of the fault are interpreted to indicate the presence of a frontal ramp (e.g. Woodward, 1987). The subjective nature of what constitutes a 'high' angle, however, makes application of this criterion difficult to implement for natural fault-related fold terminations. Because the greatest angle between the cutoff lines and fault strike will occur where the fold plunge and fault dip are steepest, we can use the model terminations derived previously for 'steep' plunges to help constrain a maximum 'high' angle for trends of cutoff lines. Specifically, if we assume maximum footwall ramp cutoff angles of 30 and 60° (Suppe, 1983; Suppe and Medwedeff, 1990) and maximum plunges of 20 and 50° for simple fault-bend and

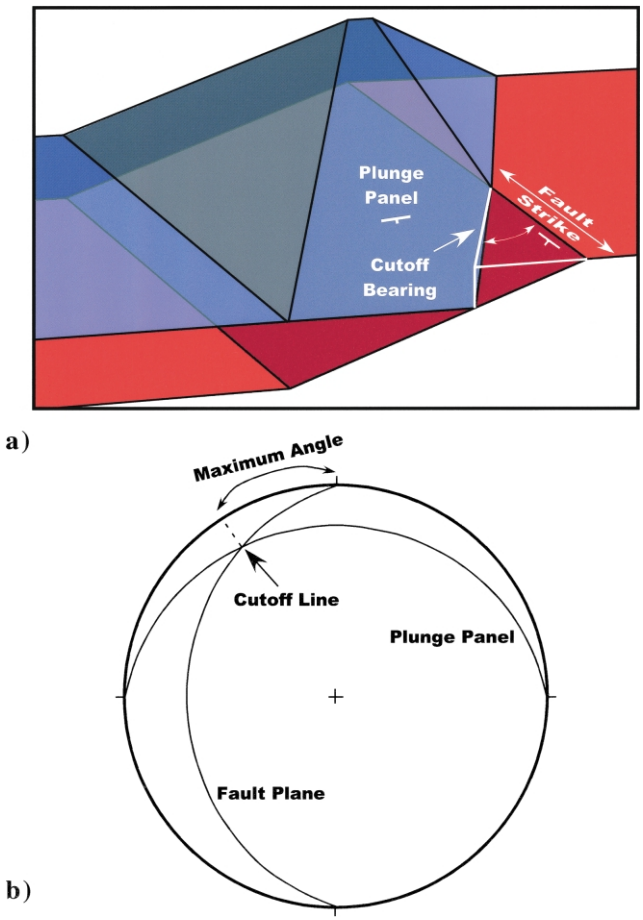

Fig. 6. (a) Three-dimensional block diagram of a cutoff line for a model fault-bend fold termination. To constrain the maximum angle (in a horizontal plane) between the fault strike and the bearing of a cutoff line for a surface in a plunging fault-related fold termination that might be produced by a displacement gradient, we find the intersection of the fault plane with the maximum plunge panel for that fault-related fold termination. For simple fault-bend folds with a constant fault geometry and a displacement gradient, the maximum plunge panel occurs where the ramp angle is 30° (Suppe, 1983), the displacement gradient is 35° (based on natural structures; Wilkerson, 1992), and the resulting maximum plunge is 20°. For simple fault-propagation folds with a constant fault geometry and a displacement gradient, the maximum plunge panel occurs where the ramp angle is 60° (Suppe and Medwedeff, 1990), the displacement gradient is 35° (based on natural structures; Wilkerson, 1992), and the resulting maximum plunge is 50°. The strike of the plunge panel for both of these simple fault-related folds is always perpendicular to the fault strike. (b) Stereonet showing calculation of the maximum angle (in a horizontal plane) between the fault strike and the bearing of a cutoff line for a surface in a plunging fault-bend fold termination that might be produced by a displacement gradient (the same procedure holds for fault-propagation folds as well). In both cases, the cutoff lines for these idealized models may be up to ≈35° from the fault strike.

fault-propagation folds with realistic along-strike displacement gradients, respectively, then a maximum angle between the bearing of the cutoff lines and fault strike can be obtained using a stereonet (i.e. by finding the plunge and bearing of the cutoff line formed by the intersection of the fault plane with the maximum plunge panel and then determining the angle between fault strike and the cutoff line bearing; Fig. 6). Using this method, we find that cutoff lines for these ideal models may be up to 33 and 35° from the fault strike for individual fault-bend and fault-propagation folds, respectively, with displacement gradients. In contrast, cutoff lines for lateral/oblique ramps with constant displacement can theoretically trend from 0 to 90° to fault strike (e.g. Fig. 7).

Again, recognizing the caveats associated with applying results from simple geometric models to interpret natural structures, these results suggest that interpretations of terminations of natural structures based solely on hanging wall cutoff lines that trend at 'high' angles to fault strike may be ambiguous for individual fault-bend and fault-propagation folds with cutoff lines that trend at ≤33–35° to fault strike. Greater angles between cutoff line bearings and fault strike for individual fault-bend or fault-propagation fold terminations may constitute a useful criterion for suggesting the presence of a lateral/oblique ramp.

2.3. Stratigraphic contacts trend at 'high' angles to fault strike

At fault-related fold terminations, faults commonly cut upsection through younger hanging wall strata towards their tips with truncated stratigraphic contacts often trending at a 'high' angle to fault strike. These two characteristics often are cited as evidence to support an interpretation of a lateral/oblique ramp forming a scoop-shaped fault surface (e.g. Bielenstein, 1969; Goldburg, 1984). An interpretation based solely on these criteria may or may not be correct; contacts that truncate against a fault surface clearly indicate a ramp, but whether the ramp is a frontal ramp or a lateral/oblique ramp is ambiguous. This is true not only for fold terminations, but also where entire structures are steeply plunging, where folds have been decapitated, or where evidence exists for significant footwall deformation (e.g. a footwall syncline).

In order to better illustrate the geometric relationships between folded strata and the genetically-related fault at the termination, we created several pseudo-three-dimensional model terminations of simple fault-bend folds (e.g. Wilkerson et al., 1991). The model terminations include: (1) a frontal ramp with a linear displacement gradient along a fault with constant geometry (Model DG; Fig. 8a), (2) a full lateral ramp that cuts upsection from a lower to an upper detachment with constant displacement along the fault (Model FLR; Fig. 8b), (3) a partial lateral ramp that cuts upsection from a lower to an intermediate detachment with constant displacement along the fault (Model PLR; Fig. 8c), and (4) a partial lateral ramp that cuts upsection from a lower to an intermediate detachment with a linear displacement gradient along the fault (Model PLR-DG; Fig. 8d). Each model was created by first constructing serial cross-sections using GeoSec™ cross-section modeling software, with each section being slightly different in order to accommodate the displacement gradient and/or changes in

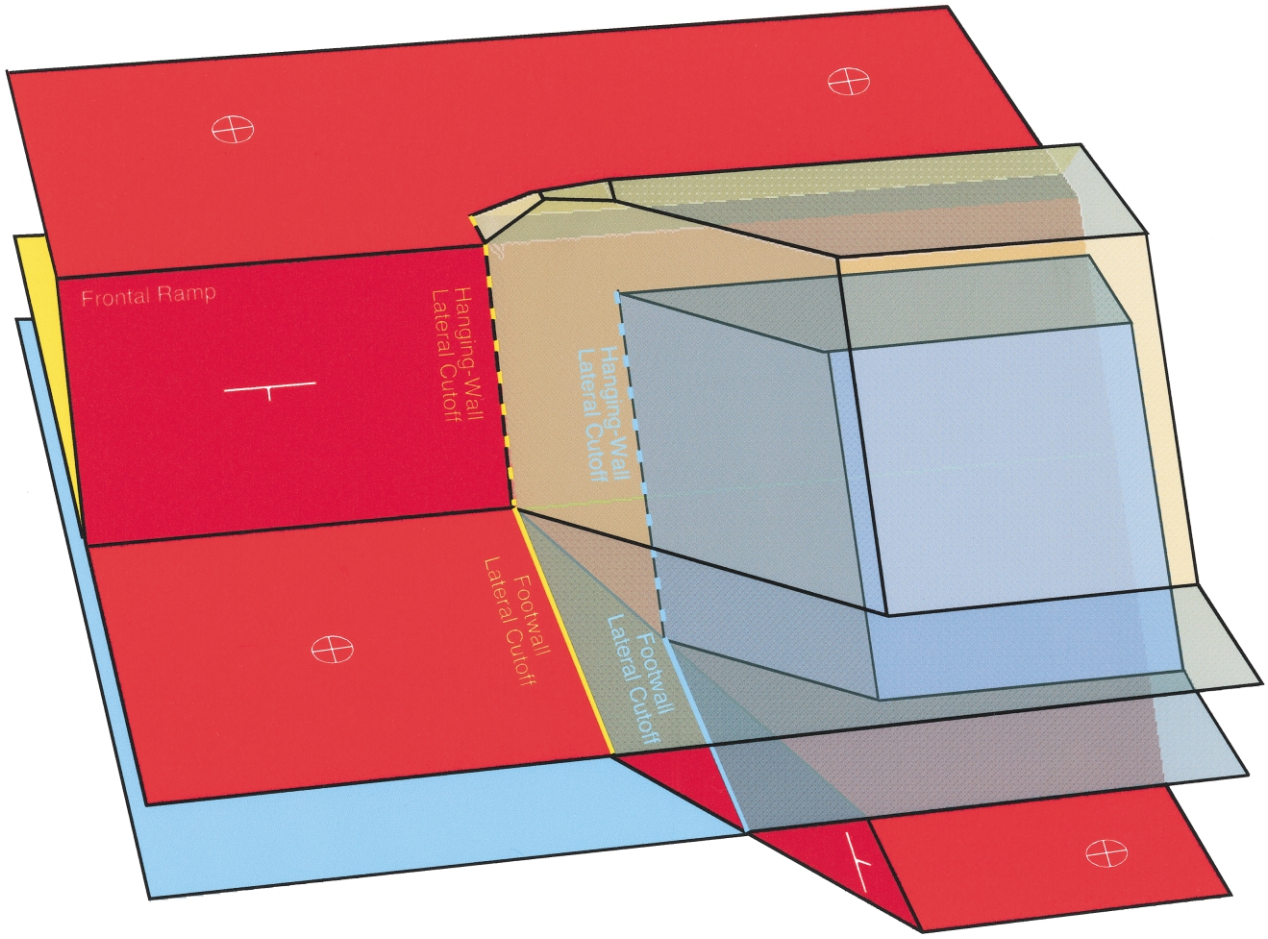

Fig. 7. Block diagram of an idealized partial lateral ramp for a fault-bend fold that cuts upsection to the left from a lower to an intermediate detachment. The lower horizon (blue) intersects the middle of the lateral ramp, and the higher horizon (yellow) intersects the top of the lateral ramp. The hanging wall lateral cutoffs (dashed colored lines) match with the corresponding footwall lateral cutoffs (solid colored lines) Layers that have not yet been displaced onto the upper flat mimic the geometry of the blue horizon, whereas layers that have been displaced onto the upper flat mimic the geometry of the yellow horizon. Dip panels in the blue and yellow surfaces that are oblique to the fault strike are produced by the decrease in ramp height while maintaining constant hinterland displacement, and the two small plunging dip panels in the yellow surface reflect fault-bend fold axial-surface geometries. Displacement is constant along strike with the transport direction perpendicular to the frontal ramp.

fault geometry necessary to simulate the appropriate model. These serial sections then were exported to GeoSec3D™ where three-dimensional surfaces were constructed by linking corresponding horizons on all the cross-sections. These three-dimensional models subsequently were exported to the gOcad™ software package where they were sliced along their various axes to produce a series of three-dimensional cutaway block diagrams that show map, strike, and dip views through the model terminations.

Analysis of the models reveals several interesting features. Model DG shows that eroded stratigraphic contacts can trend at high angles (i.e. perpendicular) to the fault surface (Fig. 8a2), thus negating the idea that stratigraphic contacts that trend at 'high' angles to fault strike indicate a lateral/oblique ramp. The lateral ramp models (Models FLR, PLR, and PLR-DG) also can possess stratigraphic contacts that trend at high angles to the fault strike (Fig. 8b1, c1, and d2). These high-angle trends are a manifestation of two characteristics specific to the lateral ramp: (1) as ramp height decreases along the strike of the fault because of the lateral ramp, more displacement is transferred to the foreland, and (2) as lateral ramp dip increases,

Fig. 8. Three-dimensional block diagrams with slices in the map, dip, and strike views (see orientation block diagram in center of figure) for the following fault-related fold terminations: (a) a frontal ramp with a linear displacement gradient along a fault with constant geometry (Model DG, $\delta = 35°$, $\Theta = 20°$), (b) a full lateral ramp that cuts upsection from a lower to an upper detachment with constant displacement along the fault (Model FLR, $\delta = 0°$, $\Theta = 20°$, lateral ramp cutoff angle = 30°), (c) a partial lateral ramp that cuts upsection from a lower to an intermediate detachment with constant displacement along the fault (Model PLR, $\delta = 0°$, $\Theta = 20°$, lateral ramp cutoff angle = 30°), and (d) a partial lateral ramp that cuts upsection from a lower to an intermediate detachment with a linear displacement gradient along the fault (Model PLR-DG, $\delta = 35°$, $\Theta = 20°$, lateral ramp cutoff angle = 30°). Inset diagrams show each footwall fault geometry with strata removed and arrows to approximate displacement on the fault. Note that the maximum displacement is not the same for each model.

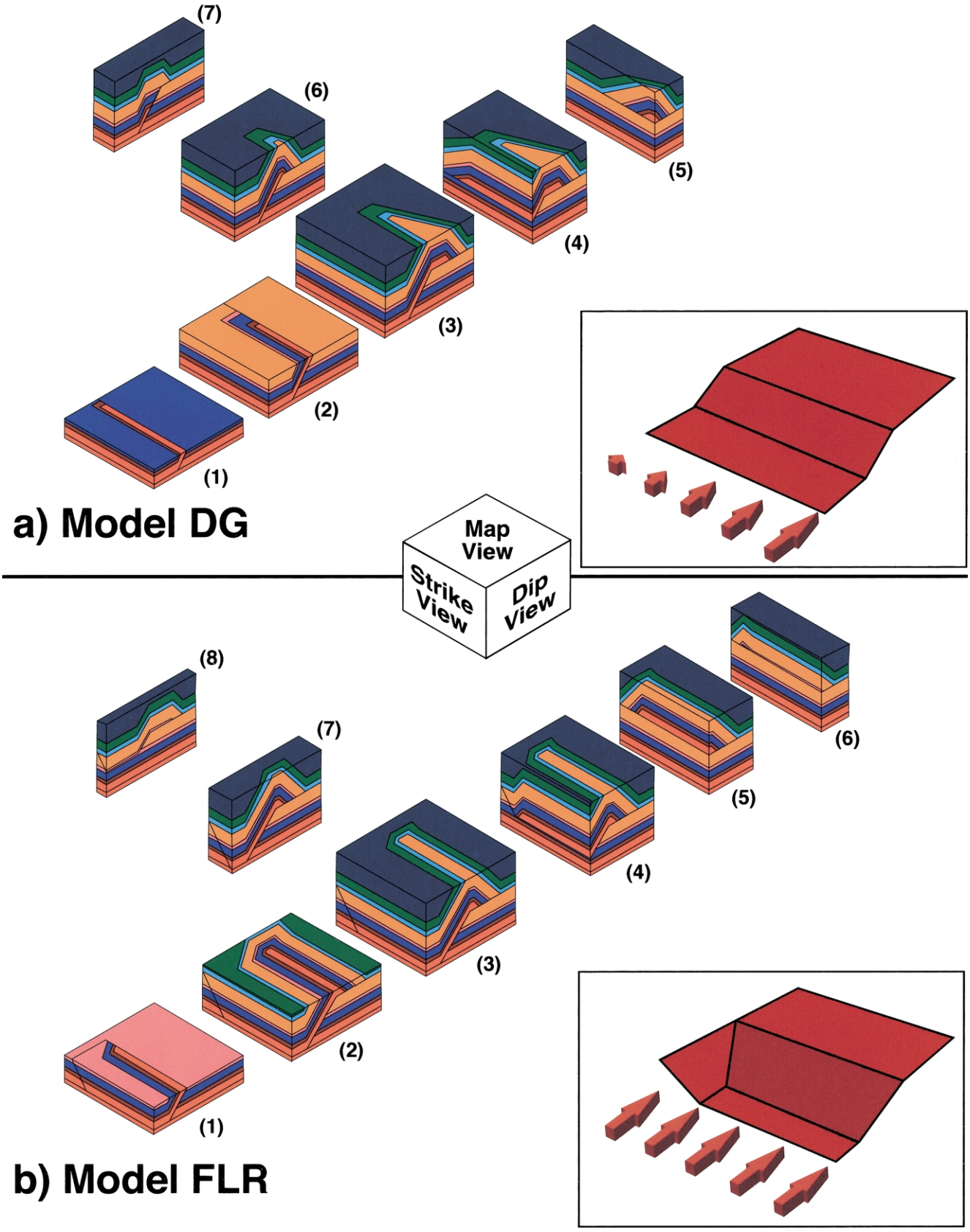
(7)
(6)
(5)
(4)
(3)
(2)
(1)
a) Model DG
Map View
Strike View
Dip View
(8)
(7)
(6)
(5)
(4)
(3)
(2)
(1)
b) Model FLR

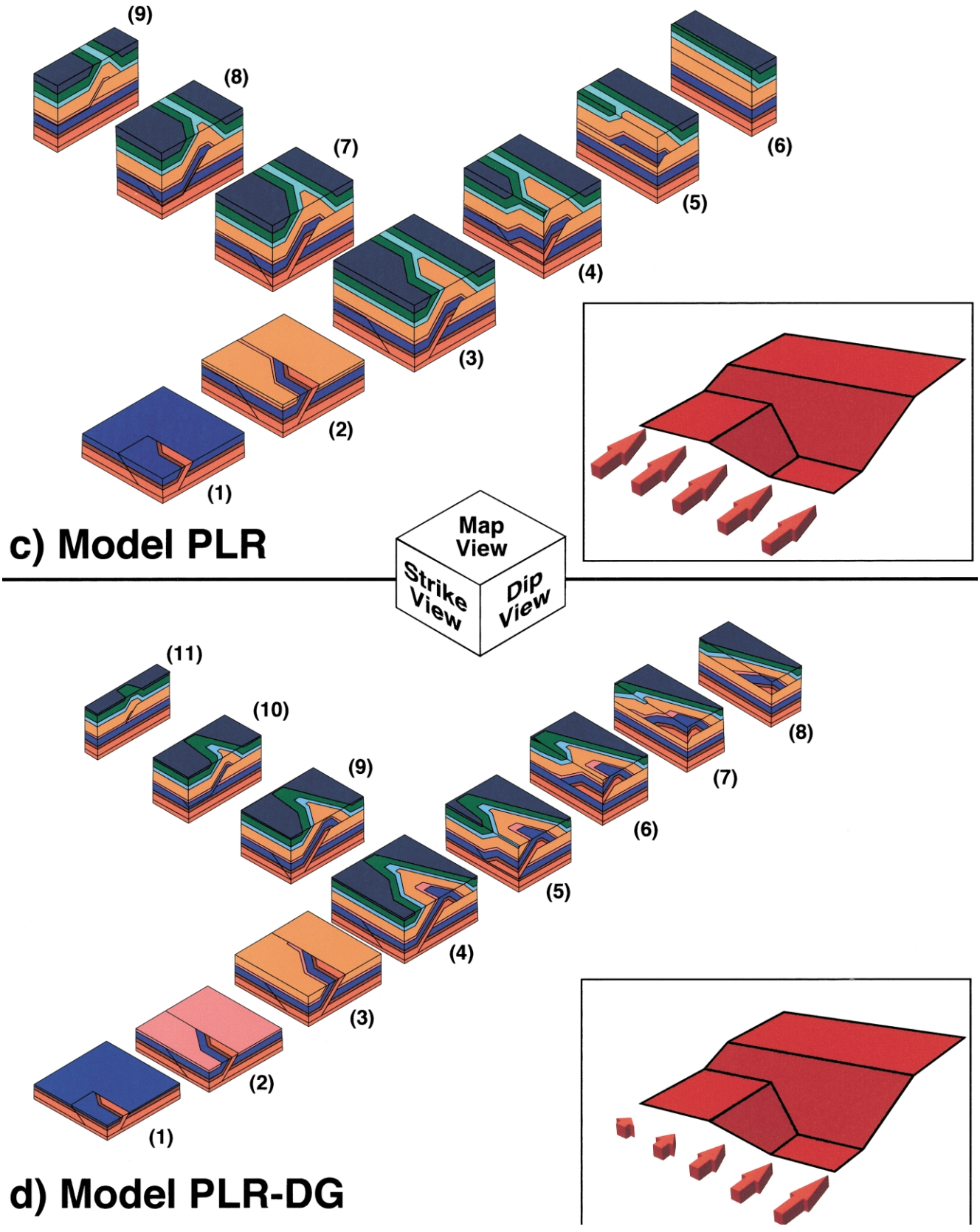

Fig. 8. (*continued*)

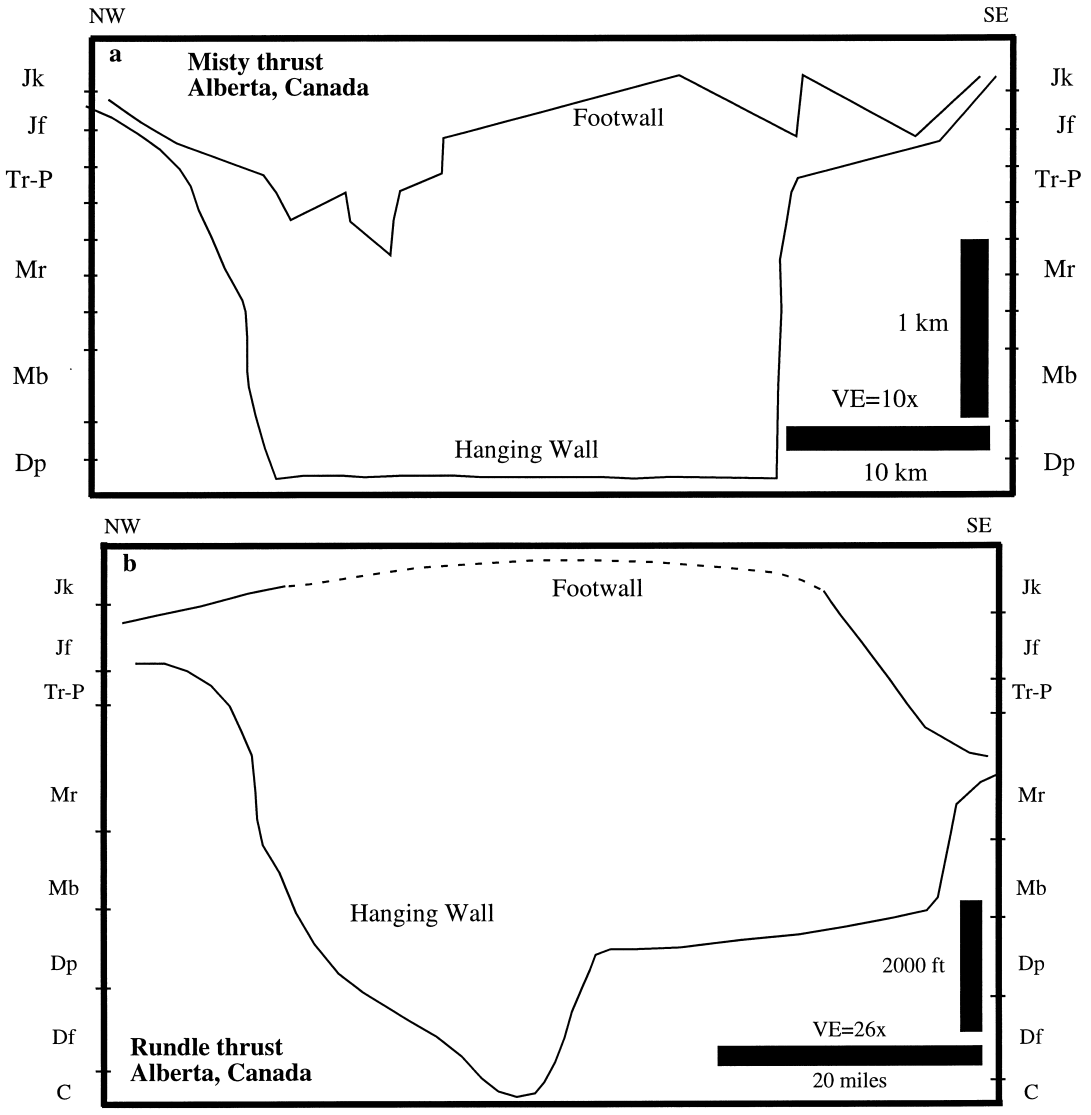

Fig. 9. Longitudinal stratigraphic separation diagrams (SSDs) for (a) the Misty thrust (modified from Castonguay and Price, 1995) and (b) the Rundle thrust (modified from Bielenstein, 1969), Alberta, Canada.

contacts strike at higher angles to the fault. Another characteristic of the geologic map pattern that might be more useful in interpreting fold terminations is the geometry of the fault trace. For Model DG, the fault trace always remains straight (Fig. 8a1 and a2), whereas for Model FLR, the fault trace always exhibits a change in trend reflecting the lateral ramp (Fig. 8b1). In contrast, Models PLR and PLR-DG display two characteristic map patterns: (1) where erosion has yet to dissect the lateral ramp, the fault trace remains straight and strata cut by the lateral ramp truncate against the fault, whereas higher strata either are parallel to the fold and then to the fault (Model PLR; Fig. 8c2) or are parallel to the fold and then trend at a very low angle to the fault and eventually terminate in a fold in response to the displacement gradient (Model PLR-DG; Fig. 8d2 and d3), and (2) where erosion has dissected the lateral ramp, the fault trace exhibits a similar geometry to Model FLR (Fig. 8c1 and d1). Although not a focus for this paper, analysis of the strike views for the various models also might be of assistance in interpreting seismic reflection strike lines to determine the nature of the termination (note that the strike-view relationships would be different for oblique ramps in that strata would show offset along the oblique ramp, whereas strata are not offset in the strike view for the lateral ramp models).

In sum, neither the presence of truncated strata near a fault tip nor the angle between the trends of stratigraphic contacts and the fault strike uniquely determine that a fault cuts upsection at its lateral tip to form a lateral ramp. Plunging folds that result solely from frontal ramps also can exhibit stratigraphic contacts that trend at a high angle to the fault traces (Fig. 8). Can the angle at which stratigraphic contacts intersect the fault strike *ever* be used to suggest a lateral/oblique ramp? Perhaps, but cautiously. In

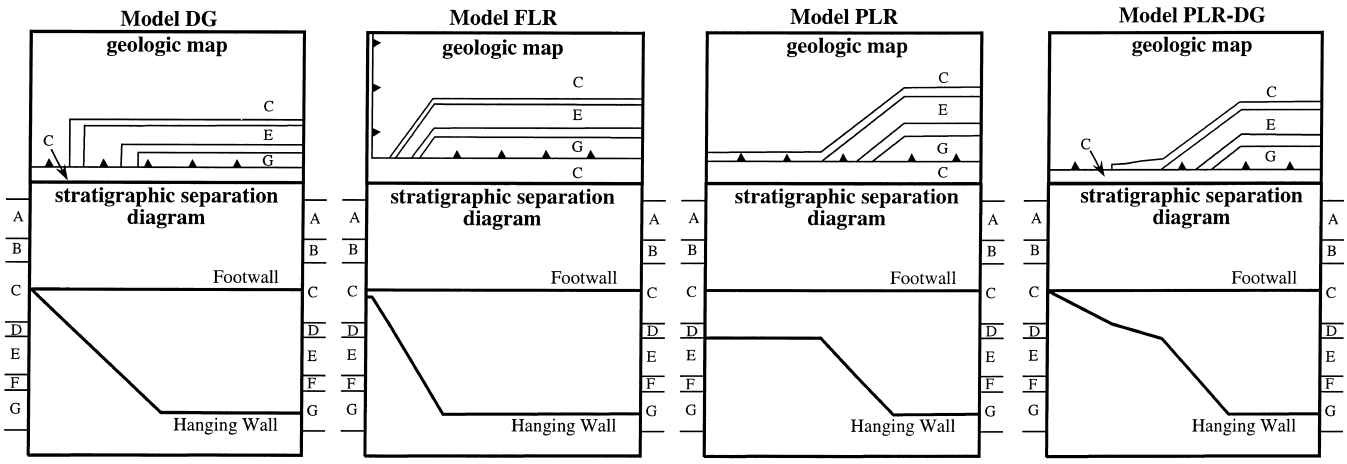

Fig. 10. Longitudinal stratigraphic separation diagrams (SSDs) for the four model terminations (colors keyed to Fig. 8; A = green, B = light blue, C = orange, D = pink, E = medium blue, F = brown, and G = light red). Model geologic maps were created at the same 'erosional' level. See text for explanation.

the middle of the thrust sheet away from fold terminations and in the absence of significant plunge, regions where there exists a transition from a long hanging wall flat overlying a long footwall flat to an abrupt ramp in the hanging wall suggests the presence of a lateral ramp in the underlying fault. However, this needs to be qualified by recognizing that a similar pattern might result from a plunging thrust sheet with a frontal ramp that is sandwiched between two hanging wall flats. Clearly, understanding the magnitude of plunge in an area and using more than one line of evidence to support an interpretation of a lateral ramp will improve the likelihood of a correct interpretation. Lastly, the along-strike relationships between the fault trace and the truncated strata also may provide insight in interpreting the fault-related fold termination, but the map pattern is highly dependent on the level of erosion and should be used with caution and in conjunction with other characteristics of the termination.

2.4. Stratigraphic separation diagrams display 'abrupt' changes near terminations

Stratigraphic separation diagrams (SSDs) plot the vertical stratigraphic position of a fault against geographic position, essentially mapping the location of hanging wall and footwall flats and ramps as a thrust cuts through the stratigraphy (e.g. Rubey, 1973; Woodward, 1987; Groshong, 1999; see Fig. 9). Woodward (1987) discussed pitfalls in interpreting SSDs when not taking local erosional re-entrants or different levels of erosion into account. He suggested that SSDs be prepared in the longitudinal (along-strike) and transport-parallel directions, utilizing cutoff lines where possible to guide the construction. As Woodward (1987) pointed out, however, transport SSDs are rare and often very short because of poor exposure parallel to the transport direction, and therefore, longitudinal SSDs are more common.

It is tempting to interpret 'abrupt' changes in stratigraphic level on SSDs near a fault-related fold termination as evidence for a lateral ramp (Fig. 9). However, abrupt changes in the hanging wall stratigraphic level on a longitudinal SSD indicates only that a hanging wall ramp exists. It does not provide any information on the geometry of the ramp (frontal or lateral). To demonstrate that SSDs are ambiguous, we constructed SSDs for Models DG, FLR, PLR, and PLR-DG (Fig. 10). Models DG and PLR-DG show that stratigraphic separation goes to zero where displacement decreases to zero, whereas Models FLR and PLR do not because of the constant displacement along strike. The only other appreciable difference between the models occurs for Model PLR-DG, which shows multiple panels in the ramp area reflecting the composite effects of both the partial lateral ramp and the displacement gradient. Using SSDs as the sole criteria for interpreting a lateral/oblique ramp at a termination, therefore, is problematic and should only be used in conjunction with other observations supporting the interpretation.

2.5. Faults exhibit actual changes in orientation

The best evidence to support the presence of a lateral/oblique ramp is the direct measurement of changes in strike of the footwall fault surface itself (in the absence of footwall deformation). Specifically, if fault segments change trend to become sub-parallel or slightly oblique to the transport direction after the removal of topographic effects, a lateral/oblique ramp, by definition, exists (e.g. Apotria et al., 1992; Apotria, 1995; Apotria and Wilkerson, 2001; see Fig. 7 for idealized example). This change in trend likely will also affect the overlying hanging wall thrust sheet as well. In particular, as the hanging wall folds over such a lateral/oblique footwall ramp, pre-existing structures may be rotated with respect to their regional orientations (e.g. joints, cleavage; Apotria et al., 1992; Wilkerson et al., 1992; Apotria, 1995; Holl and Anastasio, 1995; Dubey, 1997;

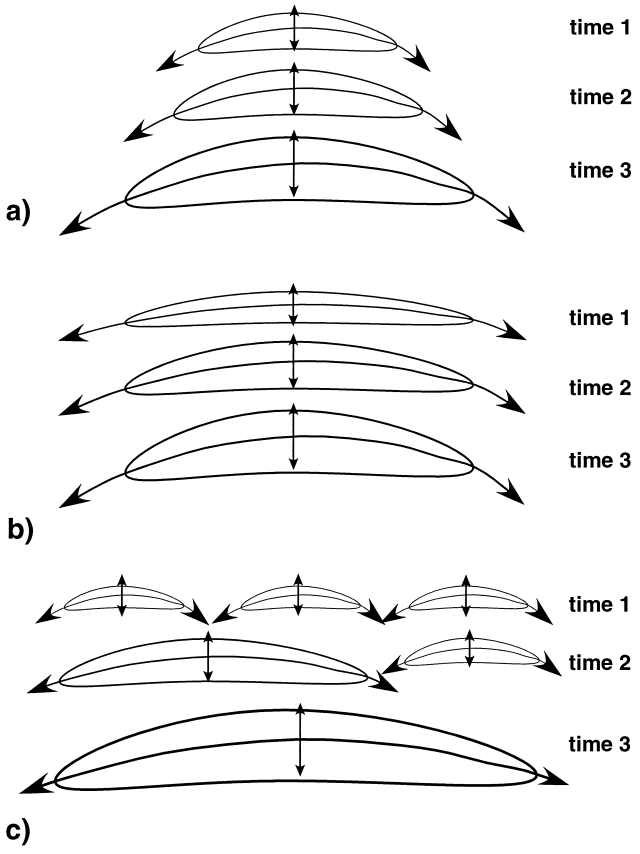

Fig. 11. Models for the lateral propagation history of a thrust fault and associated fold. (a) Structure initiated as a small feature and then propagated laterally from the center as slip increased on the underlying fault. (b) Structure began as a large, laterally continuous feature with its along-strike length set from the onset of deformation. With additional slip on the fault, the fold increased in size and amplitude. (c) Structure developed from the coalescence of many small faults that eventually linked to form a common fault surface.

Mouthereau et al., 1999). Folds and faults also may develop at a high angle to the overall transport direction, commonly with fold axes parallel to the strike of the lateral/oblique footwall ramp (Apotria, 1995). In areas where the footwall ramp is convex to the hinterland, the hanging wall thrust sheet becomes extended and forms normal faults, whereas in areas where the fault is concave to the hinterland, the hanging wall thrust sheet becomes compressed, forming thrust faults (Apotria et al., 1992; Apotria, 1995). In addition, large hanging wall lateral/oblique ramps often exhibit dramatic thickness changes, leading to formation of tear faults near transitions from a thicker hanging wall to a thinner hanging wall (e.g. Mt. Head, Canada; Douglas, 1958). Although the collective presence of these secondary structures strongly suggests a lateral/oblique ramp interpretation, many of these features also can form at terminations produced by displacement gradients (C. Connors, pers. comm., 2000). It is essential, therefore, to obtain definitive information on fault attitude to uniquely constrain the interpretation.

3. Discussion

Our goals in this paper were (1) to identify ambiguities with subjective criteria commonly used to interpret the formative mechanism for fault-related fold terminations, and (2) to better define criteria that interpreters can use to more confidently distinguish between displacement gradients and lateral/oblique ramps at such terminations. Our models also provide end-members of an initial 'library' of images of plausible fault-related fold termination geometries in map and profile view.

By understanding the range of underlying causes that produce a non-unique termination geometry, we gain insight into the lateral propagation history of fault-related folds. For example, we know that natural fault-related folds can extend laterally for miles, yet we do not fully understand how to distinguish (a) whether folds began as small structures that propagated laterally from the center as slip increased on the underlying fault (Fig. 11a), or (b) whether the structures began as large, laterally continuous features with their dimensions set from the onset of deformation (Fig. 11b), or (c) whether the structures result from the coalescence of many small faults that eventually linked to form a common fault surface (Fig. 11c). If (a) is true, we should expect to see similar deformation recorded along the entire length of the fold as the propagating termination extended laterally from the center of the structure. If (b) proves correct, however, features and deformation observed at present-day fault terminations should be unique to those parts of the fold and not observed elsewhere along the length of the fold. Model (c) would suggest that features in present-day terminations should be regularly observed in paleo-terminations along the length of the fold (Fig. 11). Such paleo-terminations also might be identified by lateral/oblique ramps within the more regional thrust sheet; such lateral/oblique structures might reflect where individual small faults that were originally offset in an en échelon manner linked together (Fig. 11c).

These models are testable by mapping and comparing mesoscopic structures along the length of natural fault-related folds, by analyzing seismicity (e.g. rupture areas and recurrence intervals over time) on actively-deforming fault-related folds, and by studying growth strata of fault-related folds that experienced syn-tectonic deposition. We are in the process of collecting data in a variety of contractional settings to determine if, and under what conditions, each model applies. If lateral/oblique ramps are common mechanisms for producing fault-related fold terminations during lateral propagation, then models (a) and (c) make it difficult for a basal detachment to continue to laterally propagate because the lateral/oblique ramp has transferred slip to a higher detachment level. For the basal detachment to laterally propagate beyond a lateral/oblique ramp termination, the fault must cannibalize the lateral/oblique ramp footwall, abandoning the lateral/oblique ramp. Depending on their three-dimensional geometry, it may, in fact, be

possible that we are mapping horses without recognizing them as paleo-terminations. If so, then horses and their lateral spacings might be clues to the overall propagation mechanics of the entire thrust system. If horses are not related to paleo-terminations, then several questions arise: (1) how are lateral/oblique ramp-based paleo-terminations expressed in existing thrust sheets?, (2) are lateral/oblique ramps actually common mechanisms for forming fault-related fold terminations?, (3) does model (b) for lateral propagation of a fault dominate in natural structures?, and (4) do lateral/oblique ramps reflect some fundamental difference along the fault (e.g. change in lithology, pre-existing structure, deformation conditions, change in the nature of the detachment, etc.) that always produces a termination which no longer can laterally propagate? Further study of fault-related fold termination geometries may significantly influence our understanding of three-dimensional kinematic and mechanical models of fold-thrust development.

4. Conclusions

Map patterns and derivative relationships commonly cited in the literature as indicating lateral/oblique ramps are not necessarily unique. Specifically, fold termination plunges of up to 20° for simple fault-bend folds and of up to 50° for simple fault-propagation folds may be produced by either a loss of displacement along strike or by a lateral/oblique ramp (depending on fault ramp dip). Higher plunge values suggest a lateral/oblique ramp interpretation. Similarly, angles between trends of cutoff lines and fault strike as high as 35° for simple fault-bend and fault-propagation fold terminations can be produced by either displacement gradients or by lateral/oblique ramps. Angles $>35°$ would make a displacement gradient interpretation less likely. Two lines of evidence should not be used to interpret a lateral/oblique ramp alone: the angle between contacts of truncated strata and fault strike and abrupt changes in slope on stratigraphic separation diagrams. Both help identify the presence of a ramp and the strata it contains, but provide little information regarding whether the feature is a plunging frontal ramp or a true lateral/oblique ramp. Lastly, measurement of true changes in fault orientation (and in mesoscopic structures in the overlying hanging wall fold) in the absence of footwall deformation suggests the presence of a lateral/oblique ramp.

We caution that the specific values presented in this paper are not sharply defined boundaries that separate the different interpretations, but rather are model-derived constraints on otherwise subjective criteria. Models are just approximations that provide insight into the geometry and development of natural structures and have their own suite of limitations associated with them (or stated another way, all models are wrong…yet some are useful; B. Tikoff, pers. comm.). That is, our simple fault-bend and fault-propagation fold models are created assuming certain kinematic and geometric boundary conditions (e.g. single ramps, non-imbricated footwalls, no global shear in hanging wall, etc.), however natural structures may not develop as prescribed by these models (e.g. folding may occur prior to ramp development, the style of fault-related folding may change along strike, second-order deformation or interaction with neighboring structures may complicate the interpretation, etc.). Because of these issues, we suggest using multiple lines of evidence to support a given interpretation for the formative mechanism(s) for a particular fault-related fold termination. Obviously, the most plausible interpretations will link subsurface seismic reflection and well data with direct measurements of fault-bedding relationships and rock fabrics. For example, in areas where high-density two- or three-dimensional seismic reflection data exist, it should be possible to explicitly define both hanging wall and footwall cutoff lines. Such information then would allow the characterization of along-strike changes in both fault displacement and fault geometry, thereby constraining the presence or absence of a lateral/oblique ramp and/or displacement gradient. In all likelihood, however, most natural fault-related fold terminations probably share components of both displacement gradients and lateral/oblique ramps, with each structure possessing contributions from both mechanisms.

Acknowledgements

Acknowledgement is made to the Donors of The Petroleum Research Fund, administered by the American Chemical Society, for support of this research (specific funding was provided by PRF Grant #33471-GB2). The authors are indebted to Paradigm Geophysical, Inc. for the use and support of GeoSec™ and GeoSec3D™ structural modeling software packages, and to Rick Allmendinger for the use of his Stereonet™ program. The authors also wish to acknowledge support from the DePauw Faculty Fellowship Program, the DePauw University Presidential Discretionary Fund, the DePauw University Summer Research Program, the Department of Geology and Geography at DePauw University, ExxonMobil Exploration Company, and ExxonMobil Upstream Research Company. Although the authors take responsibility for the interpretations presented in this manuscript, we benefitted greatly from conversations with Nick Woodward and Steve Lingrey, and from reviews by Chris Connors, Mark Rowan, and Mark Fischer.

References

Apotria, T.G., 1995. Thrust sheet rotation and out-of-plane strains associated with oblique ramps: an example from the Wyoming salient, USA. Journal of Structural Geology 17, 647–662.

Apotria, T.G., Snedden, W.T., Spang, J.H., Wiltschko, D.V., 1992.

Kinematic models of deformation at an oblique ramp. In: McClay, K.R. (Ed.). Thrust Tectonics. Chapman & Hall, pp. 141–154.

Apotria, T.G., Wilkerson, M.S., 2001. Seismic expression and kinematics of a fault-related fold termination: Rosario Structure, Maracaibo Basin, Venezuela. Journal of Structural Geology 24 in press.

Armstrong, P.A., Bartley, J.M., 1993. Displacement and deformation associated with a lateral thrust termination, southern Golden Gate Range, southern Nevada, USA. Journal of Structural Geology 15, 721–735.

Bielenstein, H.U., 1969. The Rundle thrust sheet, Banff, Alberta. Ph.D. thesis, Queen's University.

Castonguay, S., Price, R.A., 1995. Tectonic heredity and tectonic wedging along an oblique hanging-wall ramp: the southern termination of the Misty thrust sheet, southern Canadian Rocky Mountains. Geological Society of America Bulletin 107, 1304–1316.

Couzens, B.A., Dunne, W.M., 1994. Displacement transfer at thrust terminations: Saltville thrust and Sinking Creek anticline, Virginia. Journal of Structural Geology 16, 781–793.

Coward, M.P., Potts, G.J., 1983. Complex strain patterns developed at the frontal and lateral tips to shear zones and thrust zones. Journal of Structural Geology 5, 383–395.

Dahlstrom, C.D.A., 1970. Structural geology in the eastern margin of the Canadian Rocky Mountains. Bulletin of Canadian Petroleum Geology 18, 332–406.

Dixon, J.M., Liu, S., 1992. Centrifuge modelling of the propagation of thrust faults. In: McClay, K.R. (Ed.). Thrust Tectonics. Chapman & Hall, pp. 53–69.

Douglas, R.J.W., 1958. Mount Head Map Area, Alberta. Geological Survey of Canada Memoir 291.

Dubey, A.K., 1997. Simultaneous development of noncylindrical folds, frontal ramps, and transfer faults in a compressional regime: experimental investigations of Himalayan examples. Tectonics 16, 336–346.

Elliott, D., 1976. The energy balance and deformation mechanisms of thrust sheets. Philosophical Transactions of the Royal Society A283, 289–312.

Evans, J.P., Craddock, J.P., 1985. Deformation history and displacement transfer between the Crawford and Meade thrust systems, Idaho–Wyoming overthrust belt. Orogenic patterns and stratigraphy of North-Central Utah and Southeastern Idaho. Utah Geological Association Publication 14, 83–95.

Fermor, P., 1999. Aspects of the three-dimensional structure of the Alberta Foothills and Front Ranges. Geological Society of America Bulletin 111, 317–346.

Frizon de Lamotte, D., Guezou, J.-C., Averbuch, O., 1995. Distinguishing lateral folds in thrust systems; examples from Corbières (SW France) and Betic Cordilleras (SE Spain). Journal of Structural Geology 17, 233–244.

Gardner, D.A.C., Spang, J.H., 1973. Model studies of displacement transfer associated with overthrust faulting. Bulletin of Canadian Petroleum Geologists 21, 534–552.

Goldburg, B.L., 1984. Displacement transfer between thrust faults near the Sun River in the Sawtooth Range, northwestern Montana. Montana Geological Society 1984 Field Conference, 211–220.

Groshong Jr, R.H., 1999. 3-D Structural Geology. Springer, Berlin, Heidelberg.

Hennings, P.H., Prine, B.H., Wickham, J.S., 1996. 3D structural analysis and visualization of oblique-ramp accommodation structures in thrust sheets. American Association of Petroleum Geologists Abstracts with Programs.

Holl, J.E., Anastasio, D.J., 1995. Kinematics around a large-scale oblique ramp, southern Pyrenees, Spain. Tectonics 14, 1368–1379.

House, W.M., Gray, D.R., 1982. Displacement transfer at thrust terminations in Southern Appalachians—Saltville thrust as example. American Association of Petroleum Geologists Bulletin 66, 830–842.

Hyett, A.J., 1990. Deformation around a thrust tip in Carboniferous limestone at Tutt Head, near Swansea, South Wales. Journal of Structural Geology 12, 47–58.

Liu, S., Dixon, J.M., 1991. Centrifuge modelling of thrust faulting: structural variation along strike in fold-thrust belts. Tectonophysics 188, 39–62.

Mouthereau, F., Lacombe, O., Deffontaines, B., Angelier, J., Chu, H.T., Lee, C.T., 1999. Quaternary transfer faulting and belt front deformation at Pakuashan (western Taiwan). Tectonics 18, 215–230.

O'Keefe, F.X., Stearns, D.W., 1982. Characteristics of displacement transfer zones associated with thrust faults. In: Powers, R.B. (Ed.). Geologic Studies of the Cordilleran Thrust Belt 1. Rocky Mountain Association of Geologists, pp. 219–233.

Price, R.A., 2001. An evaluation of models for the kinematic evolution of thrust and fold belts: structural analysis of a transverse fault zone in the Front Ranges of the Canadian Rockies north of Banff, Alberta. Submitted to Journal of Structural Geology, in review.

Prine, B.H., 1997. Three-dimensional modeling of thrust fault terminations and their associated deformation styles; Alberta, Canada. M.S. thesis, The University of Texas at Arlington.

Ratliff, R.A., 1992. Deformation studies of folding and faulting: cross-section kinematics, strain analysis, and three-dimensional geometry. Ph.D. thesis, University of Colorado.

Rowan, M.G., Linares, R., 2000. Fold-evolution matrices and axial-surface analysis of fault-bend folds: application to the Medina Anticline, Eastern Cordillera, Colombia. American Association of Petroleum Geologists Bulletin 84, 741–764.

Rubey, W.W., 1973. New Cretaceous formations in the western Wyoming thrust belt. United States Geological Survey Bulletin 1372-I.

Schirmer, T.W., 1988. Structural analysis using thrust-fault hanging-wall sequence diagrams: Ogden duplex, Wasatch Range, Utah. American Association of Petroleum Geologists Bulletin 72, 573–585.

Stockmal, G.S., 1979. Structural geology of the northern termination of the Lewis thrust, Front Ranges, Southern Canadian Rocky Mountains. M.S. thesis, University of Calgary.

Suppe, J., 1983. Geometry and kinematics of fault-bend folding. American Journal of Science 283, 684–721.

Suppe, J., Medwedeff, D.A., 1990. Geometry and kinematics of fault-propagation folding. Eclogae Geologicae Helvetica 83, 409–454.

Wheeler, R.L., 1980. Cross-strike structural discontinuities: possible exploration tool for natural gas in the Appalachian overthrust belt. American Association of Petroleum Geologists Bulletin 64, 2166–2178.

Wilkerson, M.S., 1992. Differential transport and continuity of thrust sheets. Journal of Structural Geology 14, 749–751.

Wilkerson, M.S., Wellman, P.C., 1993. Three-dimensional geometry and kinematics of the Gale–Buckeye thrust system, Ouachita fold-thrust belt, Latimer & Pittsburg Counties, Oklahoma. American Association of Petroleum Geologists Bulletin 77, 1082–1100.

Wilkerson, M.S., Marshak, S., 1997. Fold-thrust belts—an essay. In: van der Pluijm, B.A., Marshak, S. (Eds.). Earth Structure. WCB/McGraw-Hill, US Division, pp. 366–387.

Wilkerson, M.S., Medwedeff, D.A., Marshak, S., 1991. Geometrical modeling of fault-related folds: a pseudo-three-dimensional approach. Journal of Structural Geology 13, 801–812.

Wilkerson, M.S., Marshak, S., Bosworth, W., 1992. Computerized tomographic analysis of displacement trajectories and three-dimensional fold geometry above oblique thrust ramps. Geology 20, 439–442.

Woodward, N.B., 1987. Stratigraphic separation diagrams and thrust belt structural analysis. 38th Field Conference, Wyoming Geological Association Guidebook, pp. 69–77.